

Baseline Research Studies in Support of Validation or Refinement of the Adopted Texas Commission on Environmental Quality Environmental Flow Standards for the Brazos River Estuary

Methods Summary



Prepared by the Environmental Institute of Houston University of Houston - Clear Lake in cooperation with the Texas Water Development Board





**Prepared by the Environmental Institute of Houston /
University of Houston-Clear Lake**

Jenny Oakley, Ph.D., Associate Director, Research Programs
Marc Mokrech, Ph.D., Geospatial Scientist

Principal Investigator

George Guillen, Ph.D.
Environmental Institute of Houston
University of Houston Clear Lake
2700 Bay Area Blvd
Houston, Texas 77058

**Prepared in cooperation with the Texas Water
Development Board**

Evan Turner, Project Manager
Texas Water Development Board, Surface Water Division
PO Box 13231
Austin, TX 78711

October 18, 2022

Table of Contents

Methods.....	4
<i>Historical Shoreline Changes in the Brazos River Mouth</i>	4
<i>Study Sites</i>	9
<i>Hydrology</i>	10
<i>Suspended Solids Concentration and Loading</i>	11
<i>Delineating the Brazos River Plume</i>	12
<i>Water Quality</i>	15
<i>Automated Water Quality and Water Level Meters</i>	16
<i>Nekton Collection</i>	16
<i>Nearshore Gulf of Mexico</i>	17
<i>Wetland Delta Reconnaissance</i>	17
<i>Bird sampling</i>	17
<i>Wetland Mapping</i>	21
Literature Cited	27

List of Figures

Figure 1. General location of the mouth of the Brazos River.	5
Figure 2. The 1930 and 1939 aerial photos of the Brazos river mouth.	6
Figure 3. Shoreline changes at the mouth of the Brazos river between 1850 – 2001.....	7
Figure 4. Shoreline changes at the Brazos River’s mouth and nearby coastline.	8
Figure 5. Ground Coverage of the Landsat 8 image at Path 25 and Row 40.....	12
Figure 6. The water area mask and the RGB 01/27/2015 Landsat 8 image.	14
Figure 7. Example of the delineated plume in the 01/27/2015 Landsat 8 image.....	15
Figure 8. Workflow for assessing the use of sUAS in bird sampling.....	18
Figure 9. Screenshot of the FMV application showing the flight track, the ground coverage of a video frame, and the digitized locations of birds.....	20
Figure 10. NAIP 2018 classified image using the Maximum Likelihood supervised classification method with five main wetland classes.	22
Figure 11. Woody debris in a classified NAIP 2018 image compared to a high resolution sUAS ortho image showing a good match.	23
Figure 12. Screenshot of the camera positions at the first sampling site. The blue points represent the GPS camera positions, while the green points represent the calibrated camera positions. The screenshot shows tie points that can be identified on overlapped images.	24
Figure 13. Sampling sites for producing orthoimages near the mouth of the Brazos river.	25
Figure 14. sUAS orthoimage and its classified image using the Maximum Likelihood classification method.	26

List of Tables

Table 1. List of study sites and their geographic location including approximate distance from the mouth (RKM; + upstream, - downstream into the Gulf of Mexico).....	10
Table 2. The seven bands of Landsat 8 image used in the analysis.....	13
Table 3. A list of the 13 identified bird species and their four-character codes.	19

Methods

Historical Shoreline Changes in the Brazos River Mouth

The Brazos river is the 11th longest river in the United State with 1280 miles of length from its headwater source at the head of Blackwater Draw, Roosevelt County, New Mexico to its mouth near Freeport at the Gulf of Mexico. The Brazos river proper is considered to begin where the Double Mountain and Salt Forks merge together in northeastern Stonewall County and then flows 840 miles across Texas. It is the second largest river basin in Texas with about 42,865sq miles. The mouth of the Brazos river has changed over time. According to the Brazos River Authority, the original mouth of the Brazos River once was located near the coastal towns of Surfside and Quintana. The current river's mouth moved few miles down the coast when the U.S. Army Corps of Engineers dug the new mouth in 1929 to overcome the sandbar issue, which fluctuated in depth from 4 to 10 feet, making the area impassable at the old river's mouth. A dam was built to divert the Brazos to this new outlet, where it meets the Gulf to this day (see Figure 1 for a general location of the Brazos river mouth). The 1930 and 1939 aerial photos shown in Figure 2 shows the state of the Brazos mouth after river diversion with a dam built north west of Freeport. It also shows a significant amount of sediment eroded from the old mouth and deposited at the new mouth. A dataset obtained from USGS and the Bureau of Economic Geology (BEG), at The University of Texas at Austin for the period 1850-2001 (Figure 3) shows that the shoreline in this area has changed significantly over time and it is consistent with the above brief description.

At the Texas scale, a 2011 study conducted at BEG on shoreline change rates used a series of shoreline positions including those depicted on 19th century topographic charts at selected areas, aerial photographs from 1930 to 2007, ground GPS surveys, and airborne Lidar surveys. This study found that the net shoreline retreat occurred along 84 percent of the Texas Gulf shoreline, resulting in an estimated net land loss of 5,621 ha since 1930 at an average rate of 73 ha/yr. It also found that the rates of shoreline change are more recessional on the upper Texas coast (-1.6 m/yr east of the Colorado River) than they are on the central and lower coast (-1.0 m/yr from the Colorado River to the Rio Grande). Although significant net shoreline advance occurred near the mouth of the Brazos River, notable nearby areas are undergoing significant net shoreline retreat (Paine et al. 2011). In this context and focusing on the Brazos river's mouth and nearby coastline, a visual inspection of recent historical imageries of the site were conducted and the shorelines between 2006 -2018 were digitized at 2-4-year time interval in the Google Earth platform (Figure 4). The shorelines at the river mouth have retreated but also went through cycles of growth and retreat. Moving away from the river's mouth there is a clear trend of retreat identified which is consistent with the BEG's studies of shoreline changes.

General Location of the Mouth of the Brazos River

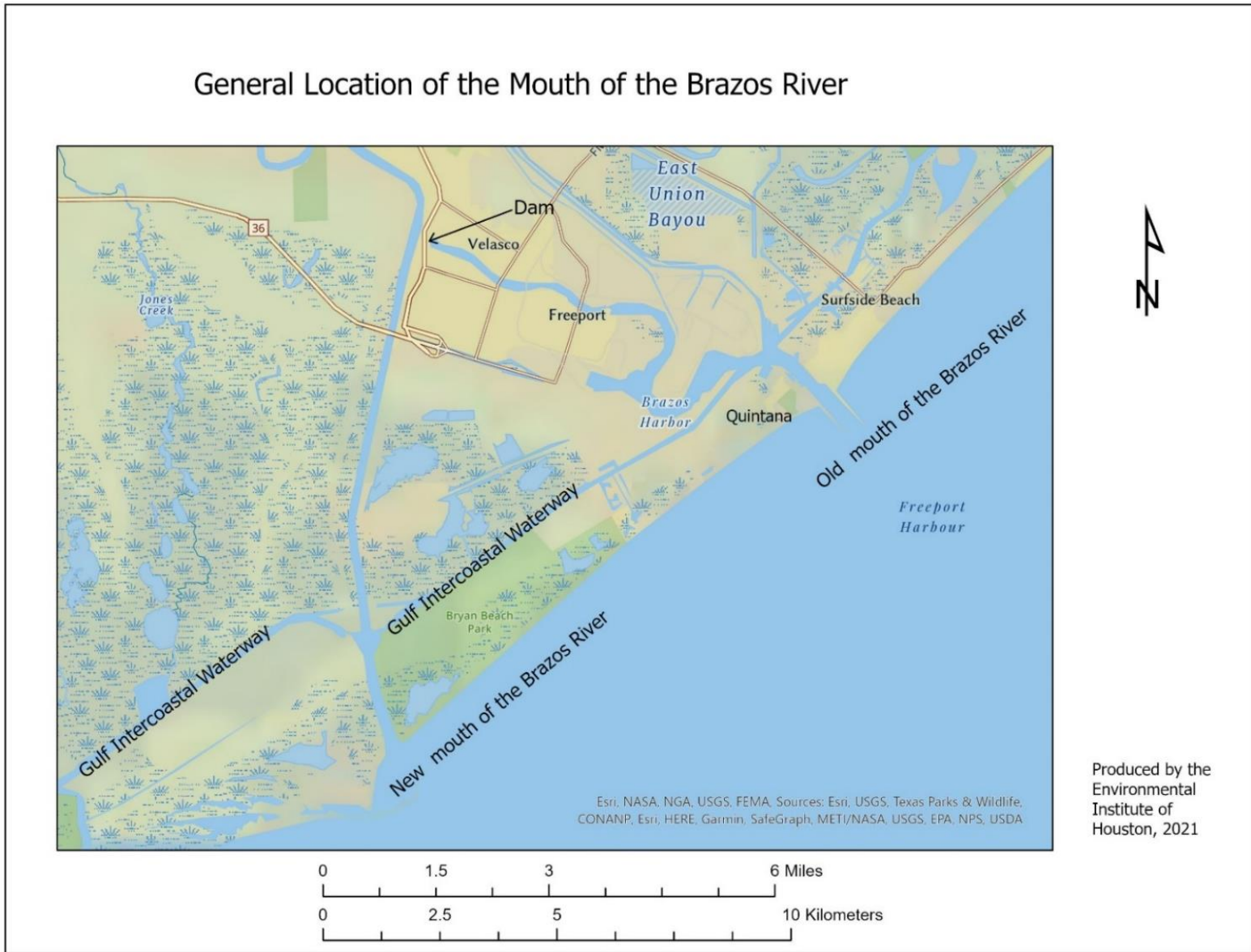


Figure 1. General location of the mouth of the Brazos River.

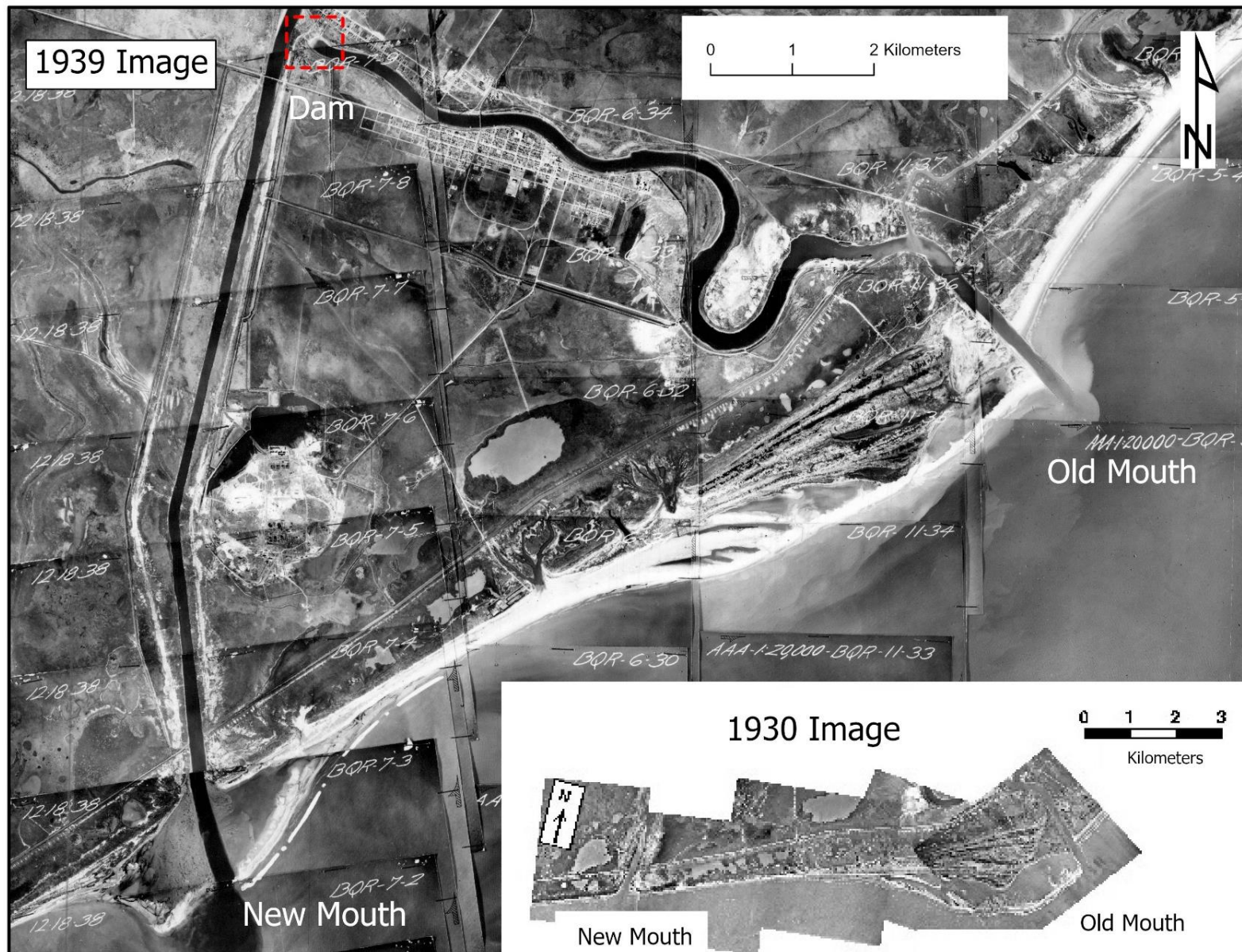


Figure 2. The 1930 and 1939 aerial photos of the Brazos river mouth.

Historical Shoreline Changes at the Mouth of the Brazos River between 1850-2001

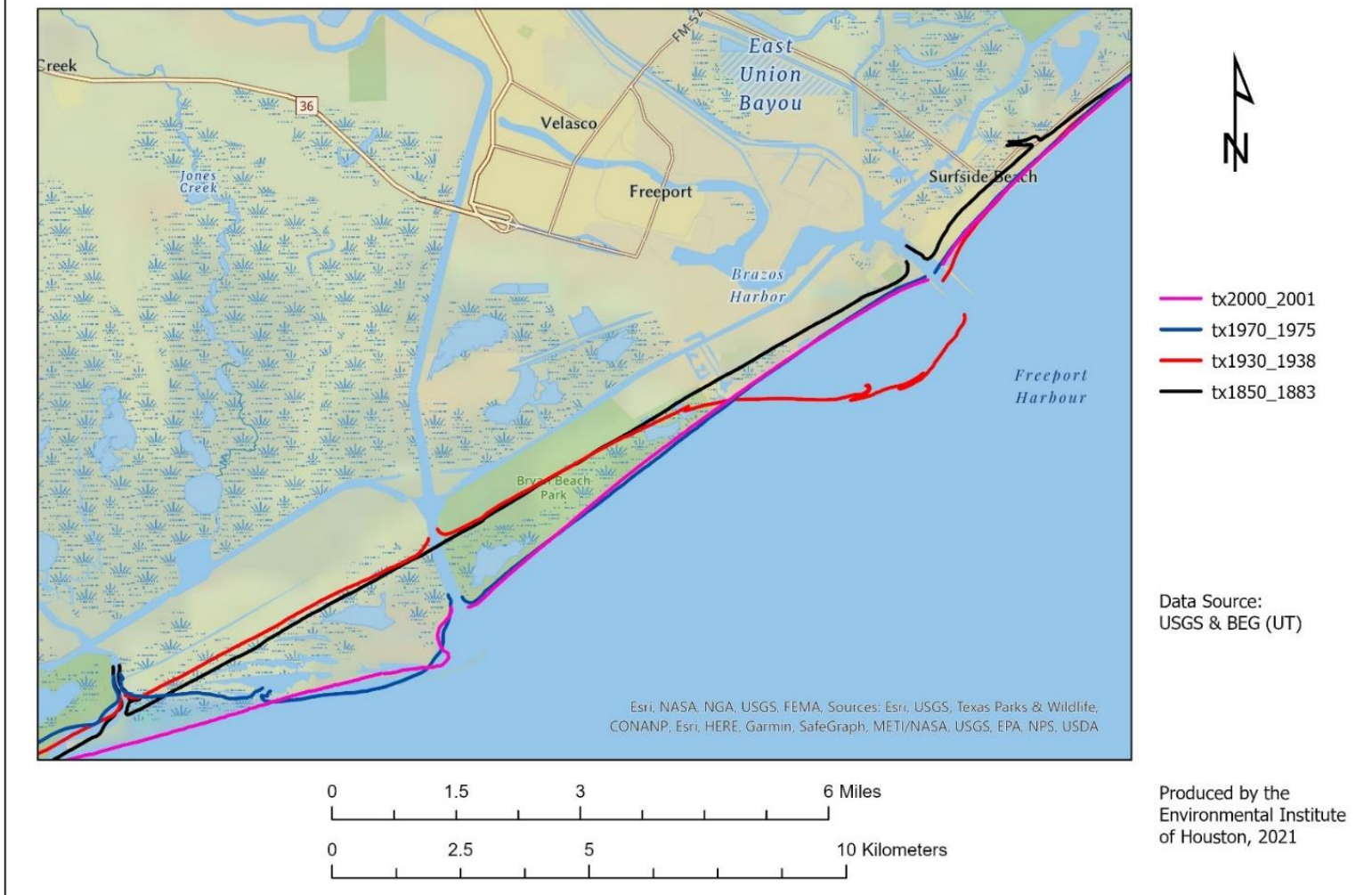


Figure 3. Shoreline changes at the mouth of the Brazos river between 1850 – 2001.



Figure 4. Shoreline changes at the Brazos River's mouth and nearby coastline.

Study Sites

The tidal portion (TCEQ segment 1201) of the Brazos River is classified as the first 25 miles (40.2 km) from its confluence with the Gulf of Mexico in Freeport, Texas, to a point about 100 m upstream of SH 332 in Brazoria County (TCEQ 2004). The tidal portion of the Brazos River can be described as a riverine or deltaic type estuary (Dyer 1997, Savenije 2005). The lower Brazos River exhibits oligohaline (low salinity-freshwater) conditions with significant variation associated with freshwater inflow (Orlando et al. 1993). The tidal portion of the Brazos River is currently classified as an unimpaired waterbody with a high rating for aquatic life use (State of Texas 2014a). The riparian ecosystem of the lower Brazos River is defined by low coastal plain vegetation transitioning from freshwater bottomland hardwoods in the upper reach to primarily saltmarsh vegetation in the lower reach (Vines 1984, Dahm et al. 2005). The channel is relatively wide (>50 m along most of its length) with the average depth gradually increasing from the mouth (4.65 m) to the upper reach (42 km) of the sampling area (7.23 m) (Miller 2014, Bonner et al. 2015).

During September 2018 to November 2020, a total of twelve sampling events of the lower Brazos River were conducted at multiple monitoring sites (Table 1). This included four primary monitoring sites at approximately 1, 10, 22, 31, and 42 river kilometers (rkm) upstream from the mouth (sites B01, B10, B22, B31, and B42 respectively). All of these sites corresponded with locations of previous surveys of the lower Brazos River conducted during 2011-2012, 2014-2015, and 2016-2017 (Miller 2014, Bonner et al. 2015, Bonner et al. 2017). Each primary site was sampled for water quality, nutrients, nekton, and zooplankton during every sampling event (except for B42, at which only water quality was sampled). Additionally, four secondary monitoring sites that were established at approximately 5, 15, 25, and 36 rkm upstream from the mouth in the 2014 study (sites B05, B15, B25, and B36, respectively) were sampled for instantaneous water quality. Continuous monitoring sites were established at 10, 21, and 35 rkm upstream of the mouth beginning in August 2018, and finally retrieved at the end of 2019. Unique to this study period was the establishment of ten study sites in the nearshore Gulf of Mexico in order to assess how freshwater inflow influences the nearshore waters of the Brazos River estuary. All ten sites were sampled for water quality, three of these ten sites also were sampled for nutrients and nekton.

Table 1. List of study sites and their geographic location including approximate distance from the mouth (RKM; + upstream, - downstream into the Gulf of Mexico).

Site	RKM	Latitude	Longitude	Site Type
G03	-3	28.8457	-95.37090	Primary
G02U1	-3	28.86508	-95.35820	Secondary
G02D1	-3	28.85212	-95.38660	Secondary
G02	-2	28.85813	95.37266	Primary
G01U3	-4	28.89297	-95.33380	Secondary
G01D3	-4	28.85201	-95.41690	Secondary
G01U1	-2	28.87510	-95.36160	Tertiary
G01D2	-3	28.84946	-95.40020	Secondary
G01D1	-2	28.8628	-95.38800	Tertiary
G01	-1	28.86862	-95.37580	Primary
B01	1	28.88368	-95.38227	Primary
B05	5	28.92592	-95.38534	Secondary
Lower ^a	10	28.96457	-95.37428	Continuous
B10	10	28.96682	-95.37464	Primary
B15	15	28.98117	-95.41979	Secondary
B22	22	29.00908	-95.45314	Primary
Middle ^b	25	29.03151	-95.47712	Continuous
B25	25	29.02987	-95.48269	Secondary
B31	31	29.03473	-95.50422	Primary
Upper ^a	36	29.04816	-95.53421	Continuous
B36	36	29.04785	-95.53343	Secondary
B42	42	29.07288	-95.57167	Secondary ^c

^a First utilized in Bonner et al. 2017; listed coordinates reflect current study as they were different in previous sampling years.

^b First utilized in Bonner et al. 2015; listed coordinates reflect current study as they were different in previous sampling years.

^c B42 was a primary site prior to current study but was downgraded to a secondary site due to previous studies showing low abundances of estuarine nekton. Grab samples were still collected at B42 in addition to vertical water quality profile readings.

Hydrology

Instantaneous and daily average freshwater inflow data was obtained from the USGS Rosharon gage throughout the study period. The Rosharon gage is the official point for determination of compliance with environmental inflow standards for the estuary (TCEQ 2014). River discharge was also calculated in the field at site B42 (river kilometer 42). Calculation of river discharge at site B42 was conducted using a Sontek River Surveyor S5/M9 ADCP. The ADCP was deployed according to standardized protocol by attaching it to a floating hydroboard and towing it across the river roughly perpendicular to the flow multiple times to estimate the water velocity field and net river discharge at the point of measurement (TCEQ 2012; Mueller and Wagner 2009). These measurements were conducted to determine if a significant difference in flow exists between the Rosharon gage and the lower river. These paired data sets can also be used to develop a linear model that predicts flows in the lower river based on the upstream Rosharon gage. Stream discharge in the tidal portion of the Brazos River as it enters the Gulf of Mexico was also estimated at river kilometer 1 and 3 (B01 and B03) along with measurements of Suspended Sediment Concentration (SSC) to estimate offshore sediment loading.

Suspended Solids Concentration and Loading

Estimates of flow and SSC were used to generate SSC loads discharged to the Gulf of Mexico (Edwards and Glysson 1999). The SSC by definition does not measure bedload which are objects too large to become suspended (e.g., boulders) or fit into the sampling container, and it does not include dissolved solids which are too fine to be retained on the filter and/or generally do not settle once flow conditions are minimal or absent.

A common water quality measurement used to assess water clarity by the TCEQ is total suspended solids (TSS). Total suspended solids are typically measured by method 2540 D described in Standard Methods (Clesceri et al. 1998). A TSS sample is usually collected using a single, surface grab, and as such, is unsuitable for estimation of fluvial sediment transport (Gray et al. 2000). Since flow intensity varies with depth, it affects both the concentration and size of the sediment particles suspended at a particular depth and within an entire water column. Results of the TSS analytical method based on surface grabs produces concentration data that are negatively biased from 25 to 34 percent with respect to concurrent depth and flow integrated SSC analyses collected at the same time, and tends to vary widely with different flows at a given site (Gray et al. 2000). Therefore, paired historical measurements of stream discharge and surface TSS cannot be used to compute fluvial sediment load due to the lack of bottom water column sampling.

A widely adopted method that is used to estimate fluvial sediment transport (loading) is the collection and measurement of suspended sediment concentration (SSC), also referred to as suspended particulate matter (SPM) when describing it in unit-less terms)- which was used for this study. A SSC sample was collected using a time and volume-integrated sampler to generate a flow-weighted estimate of the suspended sediment load (Edwards and Glysson 1999). It is important to use a flow-weighted method due to the rapid settling velocity of sand fractions in a water sample (Edwards and Glysson 1999). Unlike TSS analysis which uses an aliquot of a surface water sample, SSC determination is based on a vertically-integrated flow-weighted sample. In the laboratory, both TSS and SSC measurements yield concentrations of sediment in units of mg/L. The method used for laboratory measurement of SSC is ASTM D3977-97 (American Society for Testing and Materials 2007).

This study measured river discharge using the previously described ADCP method during the collection of SSC samples at two locations near the mouth of the Brazos River (B01 and B03) and the upper river estuary (B42) for a total of three measurements. Flow measurements and SSC collection were conducted during predicted slack ebb tide conditions to reduce tidal interference. Tide stage was confirmed using independent measurements taken at the NOAA Freeport gage located east of the mouth of the Brazos River. During SSC sampling, the gates located along the intercoastal waterway (ICWW) were left open to avoid sporadic changes in the flow pattern as caused by these gates. In addition, as noted earlier, water level (paired BaroTroll and LevelTroll) pressure gages were deployed at the middle site (B21, river kilometer 21).

The B42 site is located beyond the reach of the tidal influence and was used to estimate sediment transport into the Brazos estuary. The B03 site is located upstream of the confluence with the ICWW. This site was used to assess flow and sediment transport down to the ICWW. However, due to the potentially complex interactions with flow from the ICWW it was necessary to monitor another site (B01) immediately upstream of the mouth of the Brazos River

and downstream of the confluence of the ICWW. This would enable the assessment of what percentage of flow and sediment actually reaches the Gulf of Mexico.

Delineating the Brazos River Plume

Landsat 8 (initially named Landsat Data Continuity Mission, LDCM) imageries between 2013-2020 were obtained and can be used to estimate the size of the Brazos river plumes over time. These imageries were the best available remote sensing data that can be used to conduct this analysis due to the inclusion of the water coverage at the Brazos river mouth and surrounding area. The Landsat 8 scene covers 185km cross track by 180 km along track. Figure 5 shows a screenshot of the Landsat8 scene at Path 25 and Row 40 in the Worldwide Reference System obtained from the USGS Landsat Acquisition tool (at https://landsat.usgs.gov/landsat_acq). The Landsat 8 scene outline shows a large portion of water coverage in the study area, which makes it the relevant scene for conducting this analysis. On the other hand, two sensors on the Landsat 8 spacecraft provide seasonal coverage of the global landmass at a spatial resolution of 30 meters (visible, NIR, SWIR); 100 meters (thermal); and 15 meters (panchromatic), with 11 bands in total. These sensors detect the sun’s energy that is reflected from the earth’s surface after passing through the earth’s atmosphere twice (i.e. from the sun to the Earth and back). The electromagnetic radiation travels through the atmosphere and it is subject to absorption and/or scattering by the constituent particles that exist in the atmosphere such as gases and dust. The absorption process reduces the intensity of energy with a haziness effect, while the scattering process redirects energy in the atmosphere causing an adjacent effect on neighboring image pixels. These two processes affect the quality of any satellite image and they are the main driver for performing atmospheric corrections especially when studies include comparisons between multiple satellite imageries. Applying atmospheric corrections aims to determine the true surface reflectance values as the atmospheric effects are removed.

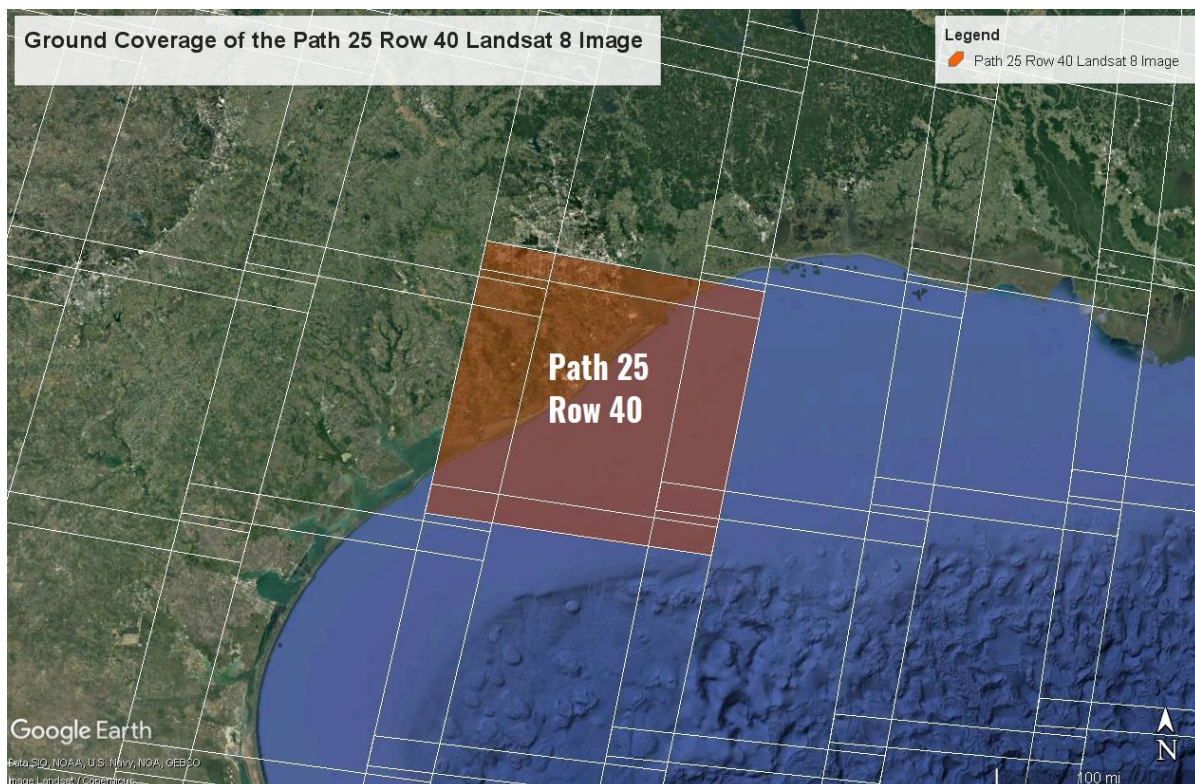


Figure 5. Ground Coverage of the Landsat 8 image at Path 25 and Row 40.

Landsat 8 Level-2 science products contain surface reflectance images that allow better investigating changes to the Earth’s environment. This dataset type was downloaded for 37 dates (Table 2) from the EarthData website at: <https://earthexplorer.usgs.gov/>. Seven bands (Table 2) of each downloaded image were used to detect and delineate the river plume of the Brazos river. The cirrus band (Band 9: 1.36-1.39 μm) is designed for better detecting of cirrus cloud contamination. It attempts to detect the light, which is reflected by the high-altitude clouds but is absorbed by the water vapor closer to the ground.

Table 2. The seven bands of Landsat 8 image used in the analysis.

Bands	Wavelength (micrometers)	Resolution (meters)
Band 1 - Coastal aerosol	0.43-0.45	30
Band 2 - Blue	0.45-0.51	30
Band 3 - Green	0.53-0.59	30
Band 4 - Red	0.64-0.67	30
Band 5 - Near Infrared (NIR)	0.85-0.88	30
Band 6 – Short Wave Infra-Red (SWIR) 1	1.57-1.65	30
Band 7 – Short Wave Infra-Red (SWIR) 2	2.11-2.29	30

The river plume analysis focusses on water cover, which is an absorbent of thermal energy. Therefore, four irrelevant bands were identified and excluded in this analysis. The excluded bands are: the panchromatic band (Band 8,), Cirrus band (band 9), and Thermal Infrared (TIRS) 1 (band 10) and Thermal Infrared (TIRS) 2 (Band11). A mask of the water cover in the Brazos River, its mouth and part of the Texas Gulf coast was generated by digitization to mask out all irrelevant land parts in the landsat 8 images. The mask extends almost 45 km on each side of the river’s mouth and 30 km off shore at the Brazos river’s mouth to ensure that large river plumes are included in the extracted datasets for this analysis. Figure 6 and Figure 7 show the mask area in the red outline with an example of the Landsat 8 image captured on 01/27/2015 and its delineated plume.

An extensive visual inspection using multiple displays of color composites combined with iso-cluster unsupervised classification at for 5, 10, 15 and 20 classes were conducted to digitize the river plumes of the Brazos river. The iso-cluster unsupervised classification method (a.k.a. ISODATA: Iterative Self-Organized Data Analysis Techniques A) uses clustering routines to create the number of classes specified by the analyst.

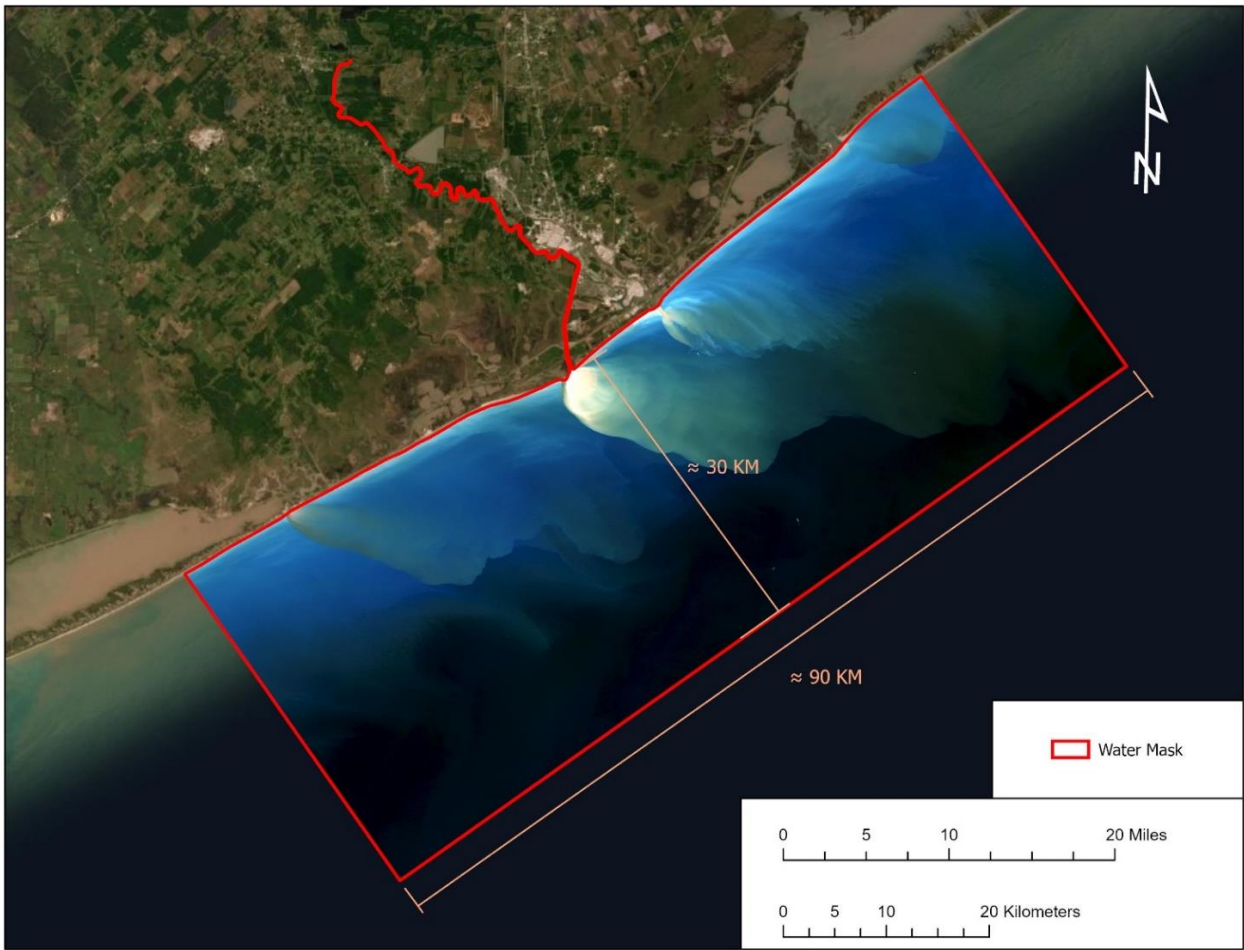


Figure 6. The water area mask and the RGB 01/27/2015 Landsat 8 image.

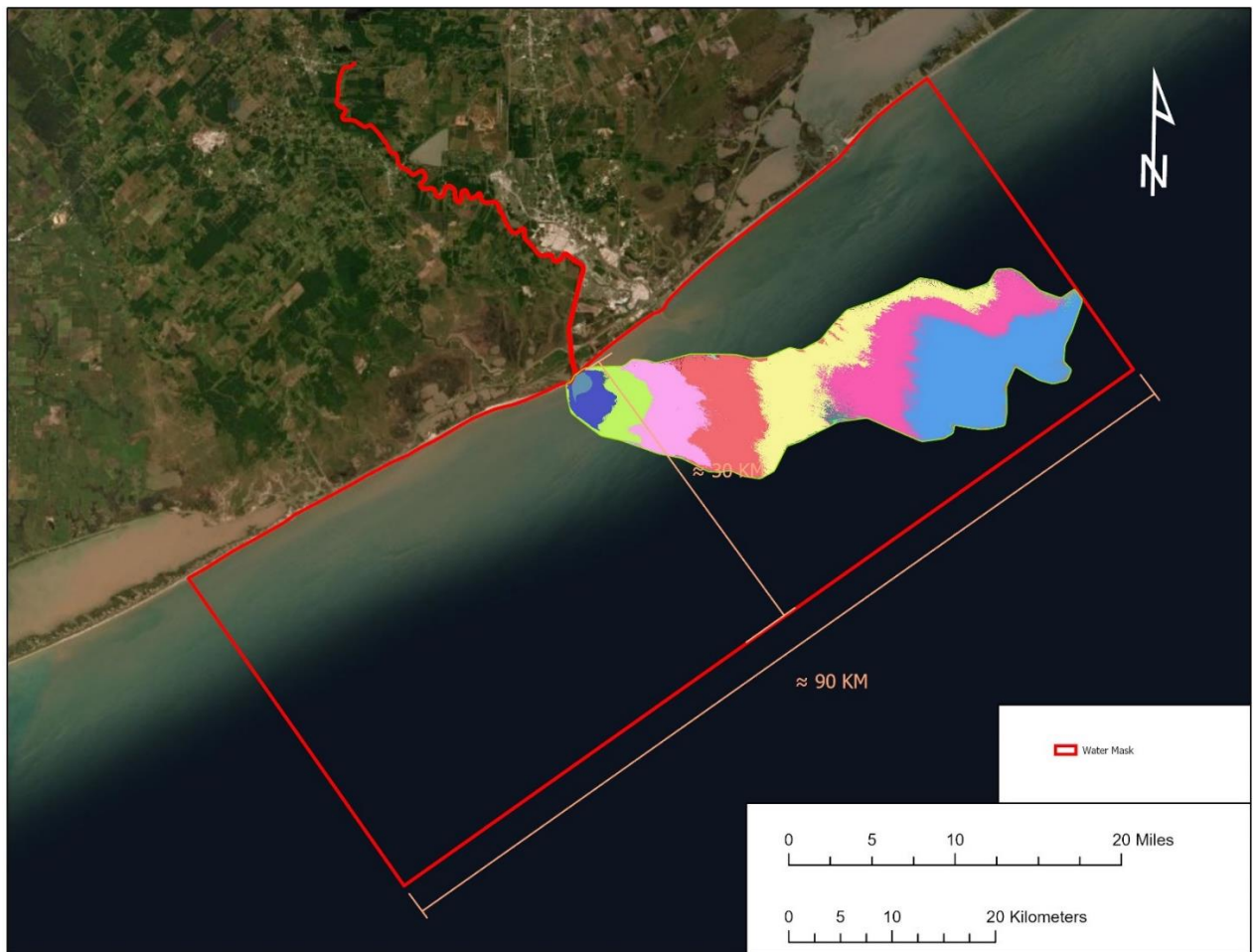


Figure 7. Example of the delineated plume in the 01/27/2015 Landsat 8 image.

Water Quality

Vertical profiles of water temperature (expressed in degrees Celsius [$^{\circ}\text{C}$]), salinity (expressed in ppt), dissolved oxygen (expressed as both % and in mg/L), pH, and turbidity (expressed in nephelometric turbidity unit [NTU]) were recorded at the thalweg of each primary and secondary sampling site using a YSI 600XLM multiprobe sonde (YSI, Inc., of Yellow Springs, Ohio). Prior to and after sampling, the sonde was calibrated according to TCEQ Surface Water Quality Monitoring quality assurance standards (TCEQ 2012). The value of each water-quality variable measured at the surface (0.3 m), 25% of total depth, 50% of total depth, 75% of total depth, and bottom (0.3 m above the bottom substrate) was recorded while conducting water quality profiles. Additionally, total depth was recorded at each site and Secchi disk transparency (depth m) was recorded at all primary sites. These same data was recorded for all ten Gulf of Mexico sites during two sampling events.

Surface water grab samples were collected at primary sites following protocol outlined in TCEQ (2012). These samples were submitted to the Eastex Environmental Laboratories of Houston, Texas for analysis. The laboratory has National Environmental Laboratory Accreditation Program (NELAP) certification for the various analytes that were measured. Nitrate and nitrite nitrogen (mg/L-N) were analyzed using EPA method SM 4500-N03 E & F. Total Kjeldahl nitrogen (TKN; mg/L-N) were analyzed using US Environmental Protection Agency (EPA) methods SM4500 SM 4500-Norg B or C and SM 4500-NH3 B. Total phosphorous (total P;

mg/L-P) were measured using EPA method SM 4500-PE. Total suspended solids (TSS; mg/L) were analyzed using EPA method SM 2540 D. The final analyte to be submitted to Eastex was chlorophyll-a, which was measured using fluorometric methods. In addition, surface water grab samples were taken at all primary and secondary sites in order to measure surface turbidity (NTU) using a nephelometer in the lab. Additional water quality samples were collected at three Gulf of Mexico sites (G1, G2, and G3).

Automated Water Quality and Water Level Meters

In addition to grab samples collected at distinct intervals in time, multiple automated ambient salinity, conductivity, dissolved oxygen, and temperature meters were also deployed to measure these variables at hourly time steps at the lower, middle and upper sites (Table 1). The continuous monitoring sites were equipped with temperature and conductivity U26-001 HOBO data loggers and dissolved oxygen sensors (Onset Computer Corporation of Bourne, Massachusetts). Data loggers were downloaded monthly and checked for battery life, fouling, and damage. Conductivity values were converted to salinity using HOBOWare (v3.7.2) to run the practical salinity scale (PSS-78) algorithm (Lewis and Perkin 1978).

Automated paired pressure transducer sensors were used to collect barometric pressure compensated measurements of water depth relative to the position of the submerged depth sensor. Paired In-Situ model Level TROLL 300 and BaroTROLL instruments were deployed at the middle site. The water depth probe, Level TROLL 300, was deployed near the river bottom, while the barometer, BaroTROLL was deployed above the water surface near the same location. The Level TROLL 300 instrument uses barometric pressure readings from the co-located BaroTROLL thermometer and barometer to correct depth readings obtained with the Level TROLL 300 (In-Situ 2013). Unpaired Level TROLL 300 instruments were also deployed at the lower and upper sites and depth-corrected using the same BaroTROLL thermometer and barometer readings at the middle site.

Nekton Collection

Nekton were collected at four of the previous sites surveyed during earlier studies. Demersal nekton were collected in the thalweg at all primary sites (B01, BIO, B22, and B31) with an otter trawl (3.1 m wide, 38.2 mm stretch mesh, 6.1 mm net fitted within cod end) towed for approximately five minutes per replicate. A total of three replicate tows were made at each site. Trawls were performed counter to flow (facing upriver) at an average speed of 2.5 knots and equipped with a thirty-meter tow line. In instances where snags prevented the full trawling allotment, catch was released and the trawl was redeployed upstream of the hazard (snag) location. Triplicate hauls were also performed at three Gulf of Mexico sites (G1, G2, and G3). Shoreline nekton was collected at all primary sites using a modified 6.4 mm mesh Renfro beam trawl manufactured by Sea-Gear Corporation of Melbourne, Florida (Renfro 1963). Triplicate hauls were pulled parallel to shore for 15.2 m/haul on one bank per site (alternating sides during each sampling event and at each site).

Collected nekton was identified to the lowest possible taxonomic level and counted. Nekton includes mobile finfish and invertebrates such as shrimp, swimming crabs, and squid. Any specimen unidentifiable in the field was anesthetized with MS-222, preserved in 10% formalin and brought back to the lab for subsequent identification and enumeration. Laboratory and field identification were conducted using a combination of expert knowledge and taxonomic keys,

and reported using common and scientific names. The number of individuals per taxa was tallied for each gear type and replicate sample.

Nearshore Gulf of Mexico

Limited monitoring of water quality and nekton (as described above) was conducted for two sampling in the nearshore waters in close proximity to the Brazos River. These sampling events were conducted during periods of low and high river flow to evaluate the response of nearshore Gulf of Mexico waters to Brazos River discharge.

Wetland Delta Reconnaissance

A limited reconnaissance and characterization of the Brazos River delta was performed over several days and using a variety of field methods. These included limited aerial over flights and shallow draft boat and foot surveys. The intent of the survey was to collect preliminary data on the major plant communities, connecting waterways, and aquatic and bird life. Vegetation plots were established in order to evaluate the percent cover and dominant plant communities present on the delta. Wading and shoreline birds were surveyed using binoculars and drone surveillance. Field identification was conducted using expert knowledge and taxonomic keys and reported using common and scientific names. All data was georeferenced using survey grade GPS.

Bird sampling

An initial assessment of the bird species at the Brazos river was conducted using the 2018 NIAP dataset and high-resolution datasets collected using sUAS. The aim of this investigation is to assess the effectiveness of using small Unmanned Vehicle System (sUAS) in bird sampling as well as determining key foraging habitat for birds. The implemented framework in Figure 8 shows the multiple stages and workflow that were conducted in the field and in post-processing at the office. As the selection of the bird sampling sites cannot be planned in advance, a field surveillance of the mouth of the Brazos river was the first stage implemented to identify the sites where birds exist on the day/time of bird sampling. This was done by navigating the mouth of the Brazos river using a surface drive vessel and visually identifying the locations birds with binoculars. Once the survey site is identified, two research teams positioned themselves on land in two adjacent spots. The conventional survey team consisted of two researchers occupied a high ground where they were able to have clear view of the birds' site. The equipment used to locate birds and identify their species using conventional method include Vortex Spotting Scope and tripod, Bushnell Fusion 1-mile ARC 12x50 mm magnification binoculars with built-in laser rangefinder, and a Compass.

The sUAS survey team consisted of two remote pilots and an observer occupied a nearby spot. Two sUAS units were used simultaneously in this survey, namely the DJI Mavic Air 2 unit with 12-megapixel camera to fly over the birds' site at 7 ft altitude without disturbing the birds. This sUAS unit flew in transects or as remote pilot sees necessary to survey the Bird-sampling site. In an effort to avoid disturbing birds, the Mavic Air 2 unit was used to transect the bird-sampling site because it is reported to be one of the quietest sUAS units on the market. A second DJI Phantom 4 Pro Quadcopter with 20-megapixel camera was positioned at much higher altitude to overlook the whole sampling site with the aim of having another source that can be used to avoid double counting birds when these birds fly over the site and change locations especially when high density of birds is encountered. Although, the birds' movement and the handling of the potential

double-counting of birds was part of the method, the results from the second (fixed) sUAS were insignificant due to the low density of birds on site in this sampling event. Thus, the results from the second sUAS unit won't be discussed further in this report.

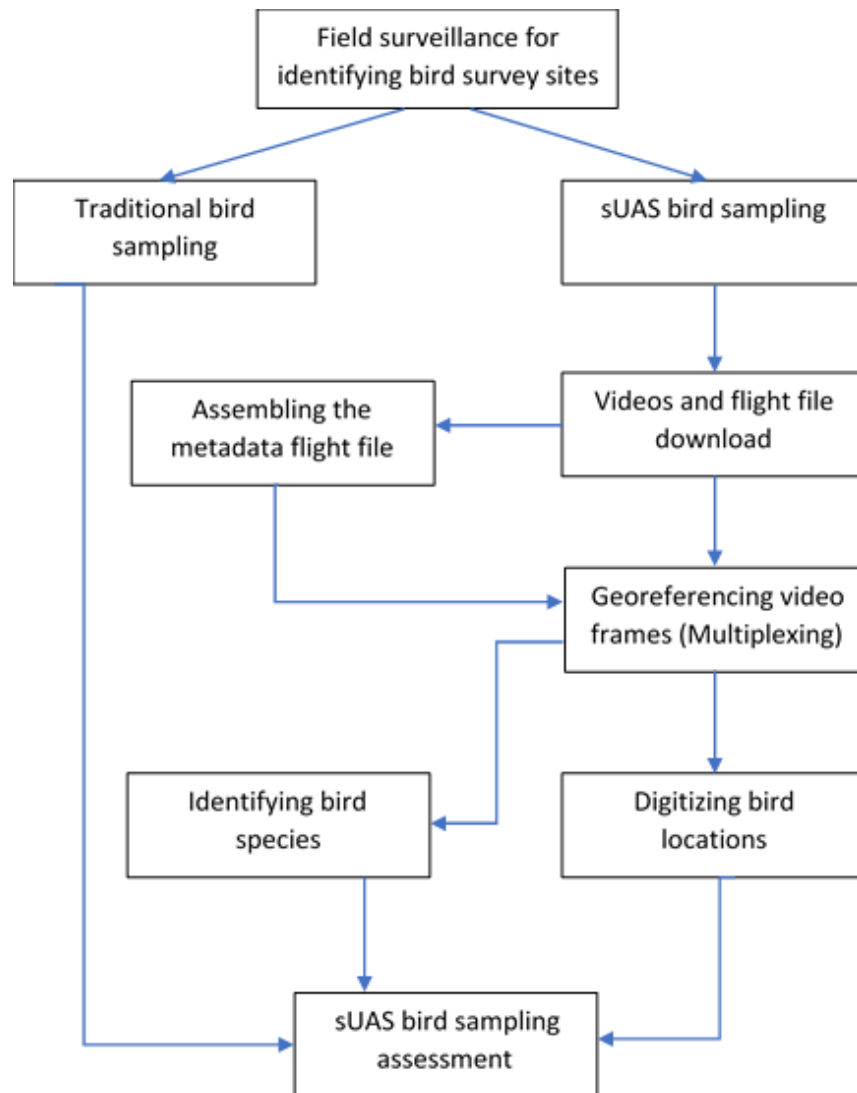


Figure 8. Workflow for assessing the use of sUAS in bird sampling.

Conventional and sUAS sampling methods were conducted simultaneously on 06/27/2019 at 9:28 am. In the conventional sampling method, the Bushnell Fusion 1-Mile ARC 12x50 mm magnification binoculars with built-in laser rangefinder and a Vortex Spotting Scope were used to spot and identify birds. Every bird sighted was recorded, including the surveyor's location (latitude, longitude), the distance to the birds, bearing of the bird from the observer's location, number of individuals of that species in the group, wind speed and wind direction. The bird's distance from observer is determined using the laser rangefinder built into the binoculars. The direction from the observer location to the recorded bird is determined using a compass. Data was entered into excel. Distance from observer to bird was converted from yards to meters. Bearing is converted from degrees into radians, and easting and northing values were calculated for each bird sighting. A total of 170 birds were observed during four flights with 13 bird species were identified in the conventional sampling method (Table 3).

Table 3. A list of the 13 identified bird species and their four-character codes.

Group	Order	Family	Bird Code	Common Name
Shorebird	Charadriiformes	Recurvirostridae	BNST	Black-necked Stilt
		Scolopacidae	WILL	Willet
Wading Bird	Pelecaniformes	Ardeidae	BCNH	Black-crowned Night Heron
			GBHE	Great Blue Heron
			GREG	Great Egret
			LBHE	Little Blue Heron
			REEG	Reddish Egret
			SNEG	Snowy Egret
			TCHE	Tricolored Heron
		Threskiornithidae	ROSP	Roseate Spoonbill
	WHIB	White Ibis		
Waterbird	Charadriiformes	Laridae	BLSK	Black Skimmer
	Suliformes	Phalacrocoracidae	NECO	Neotropic Cormorant

High definition videos were recorded using the DJI Mavic Air 2 camera. The MP4 video files with associated DAT flight files were downloaded for post processing. As this is a sampling exercise for testing the sUAS method, the videos were examined thoroughly for quality assessment and the video from the third flight was identified as the best quality video for post-processing using the Full Motion Video (FMV) capabilities in the ArcGIS Pro platform.

The FMV geoprocessing tools include the capability of seamlessly mapping features by digitizing and compiling feature data right on the video frames using the video player within the ArcGIS Pro (Figure 9). This process requires that the videos are Motion Industry Standards Board (MISB) compliant. The MISB-compliant videos consist of video frames that are captured in time and space. The display of these images in sequence, at the same rate captured, generates the motion in a video while the direct use of geo-referencing information and sensor parameters establishes the location and coverage of each image. Sensor systems that capture directly MISB-compliant videos are usually very sophisticated and expensive as they record all geo-referencing information directly on image frames including 3D position of sensor, orientation of sensor and time of recording. However, FMV enables the use of less expensive commercial off-the-shelf consumer-oriented video capture systems (such as the Mavic Air 2 system) by providing the possibility of encoding video files with the required metadata using the Video Multiplexer Geoprocessing tool. The use of the Multiplexer Geoprocessing tool requires the construction of a metadata file, which includes the following 12 parameters: Unix Time Stamp, Platform Heading, Platform Pitch, Platform Roll, Sensor Latitude, Sensor Longitude, Sensor Altitude, Sensor Horizontal Field of View, Sensor Relative Azimuth, Sensor Relative Elevation, and Sensor Relative Roll. The values of these parameters can be obtained from the flight files and from the specs of the sUAS camera.

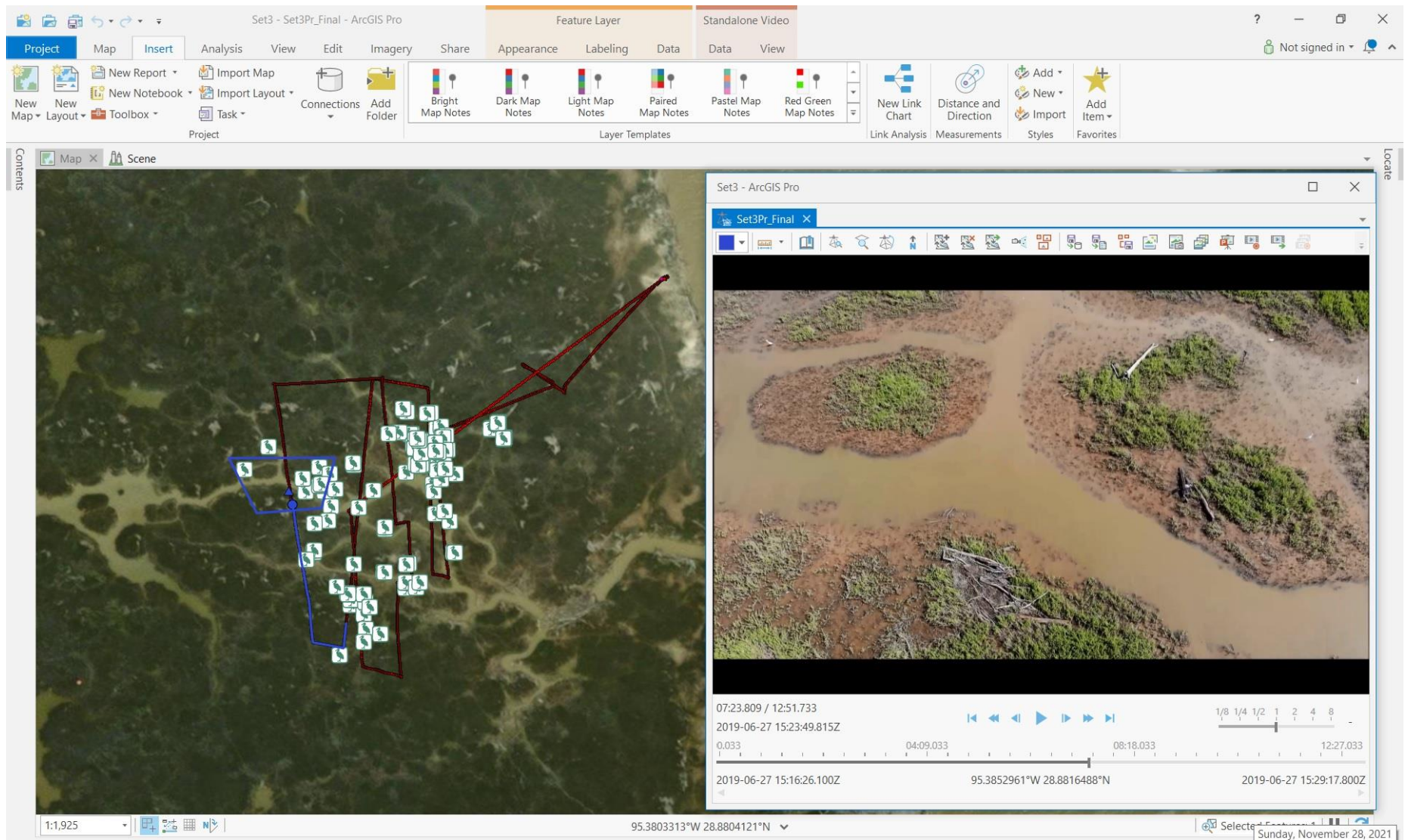


Figure 9. Screenshot of the FMV application showing the flight track, the ground coverage of a video frame, and the digitized locations of birds.

After the Multiplexing process is completed, birds were digitized directly from the synchronized image frames and identified to the lowest possible taxon. Counts from the video were then compared to those taken in the field. A total of 116 individual birds were counted from seven identified species with two individual birds were unidentifiable in the sUAS method. By comparison, 31 individual birds from 8 identified species were observed using the conventional method. The difference between these two numbers of individual birds is significant and giving the sUAS method has a clear advantage over the conventional method when analyzing bird abundance. This can be easily explained by the fact that sUAS has the capability of viewing the study site from above revealing birds that can be hidden between the vegetation cover or the micro-terrain features in the case conventional sampling method. On the other hand, a better sensor spec is recommended to improve the species identification process. For example, the DJI Mavic 2 Advanced sUAS unit includes a better camera and zoom capability that brings the sensor spec to 48MP, which can be highly beneficial in species identification compared to the 12MP sensor used in this study.

Wetland Mapping

Two datasets were used to investigate wetland habitats at the mouth of the Brazos river. Images from the National Agriculture Imagery Program (NAIP) captured in 2018 was used to investigate the possibility of mapping and identifying vegetation communities. This 2018 NAIP image was downloaded from the TRNIS Data Hub; it has 60cm spatial resolution and includes three natural color bands (RGB) and one near-infrared band. The second dataset has higher spatial resolution (i.e. a centimeter level) compared to the NAIP dataset; it was collected using a phantom 4 Pro sUAS equipped with 20MP camera on two occasions. The following two sections describe the investigation conducted to map and analyze wetland habitats at the mouth of the Brazos river.

The use of NAIP dataset: the NAIP program is administered by the USDA's Farm Service Agency (FSA). It was established in 2003 to acquire aerial imagery during the agricultural growing seasons in the continental U.S. and to construct digital orthoimages (i.e. "leaf-on" geometrically corrected image) available to governmental agencies and the public. Over time NAIP imageries were collected using different sensors and at different time cycles. NAIP 2018 image was used for investigating the possibility of classifying wetland habitats and for investigating wetland changes over a relatively short time span of 2 years.

Wetland sampling at 43 locations was conducted using 1m and 5m quadrats, where proportions of quadrats occupied by habitat species were estimated. The sampling locations were determined by classifying a NAIP image of the site using the Iso-cluster unsupervised classification method and then distributing randomly these locations using the stratified random algorithm in ArcGIS Pro. The collected sampling data at these 43 locations was used for better understanding the characteristics of the wetland habitats on site. It is also used to test the possibility of wetland classification at the habitat type level. The Maximum Likelihood supervised classification was conducted on the NAIP 2018 image using training data digitized on the screen with the help of the wetland sampling sites. Five main classes were identified including dense vegetation, vegetation, bare ground, woody debris, and open water following the main wetland classes identified in the wetland sampling process (Figure 10). The vegetation litter category was not represented due to the limited information available about this class at the sampling sites. Visual inspection of the classified NAIP 2018 image shows that the woody debris class is the least accurate class as this class appears in some areas were woody debris unexpected. However, using

the high resolution sUAS orthoimage as a reference, the woody debris on the west bank of the Brazos river was well picked up in the classification process (Figure 11).

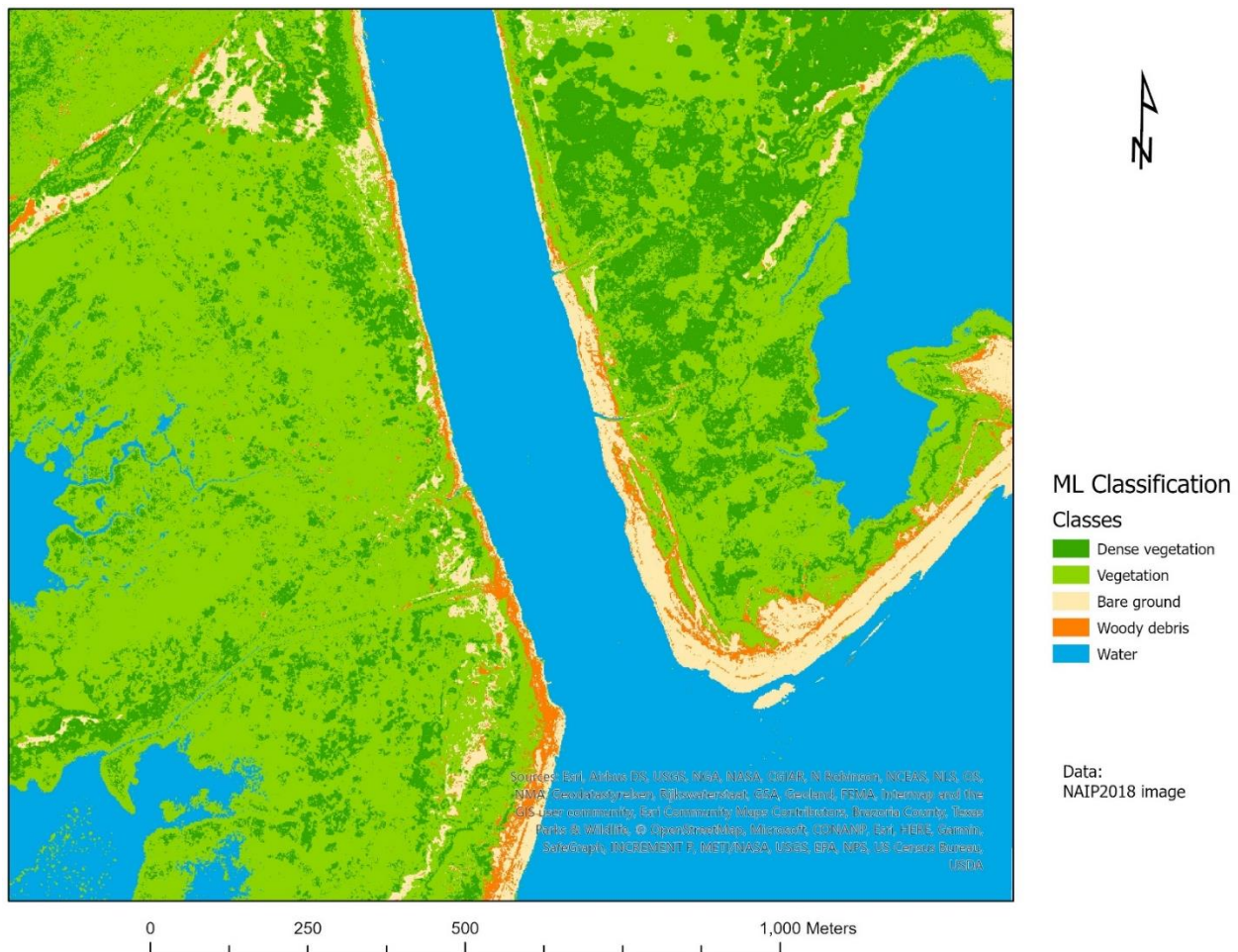


Figure 10. NAIP 2018 classified image using the Maximum Likelihood supervised classification method with five main wetland classes.

The use of sUAS dataset: overlapped images were collected using sUAS at 30 m altitude and then processed together to identify tie points that were used to construct orthoimages (Figure 12) using the Pix4D software. Geometrically corrected orthoimages with ≈ 0.9 cm spatial resolution were produced (Figure 13) and wetland habitats were analyzed at three sampling sites. The maximum likelihood supervised classification method was applied (Figure 14) to produce 5 classes: water, shallow water, woody debris, bare ground and vegetation. The vegetation litter class identified at the vegetation sampling sites was difficult to identify on the sUAS orthoimages and consequently was not possible to provide training data about this class in the Maximum Likelihood classification method. The classified sUAS orthoimage shows better classification results than the classified NAIP2018 images as the visual inspection shows significant details were picked up correctly in the classification process. The sUAS orthoimage at the bird sampling site shows light spots caused by light reflecting off shallow waters.

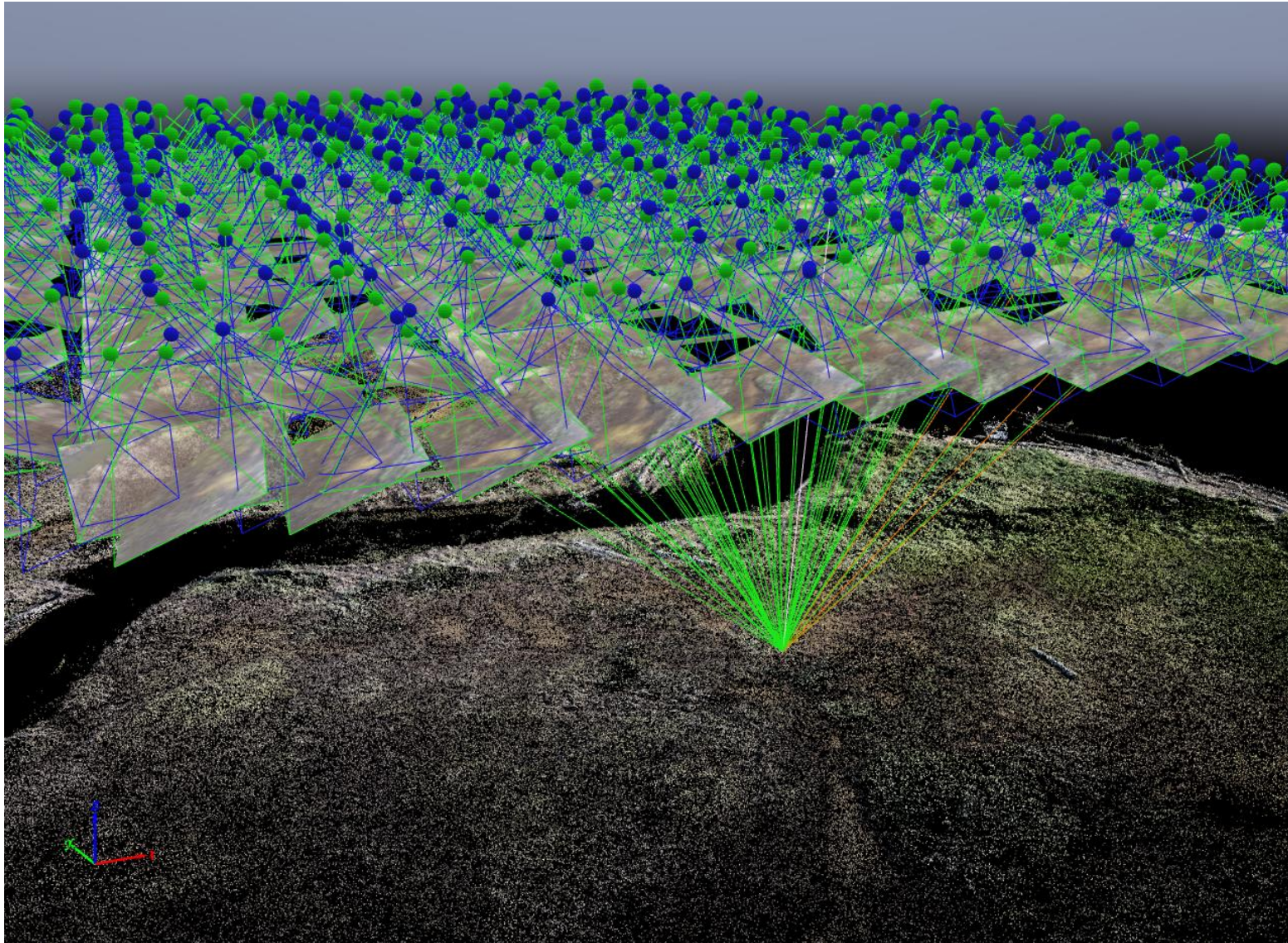


Figure 12. Screenshot of the camera positions at the first sampling site. The blue points represent the GPS camera positions, while the green points represent the calibrated camera positions. The screenshot shows tie points that can be identified on overlapped images.

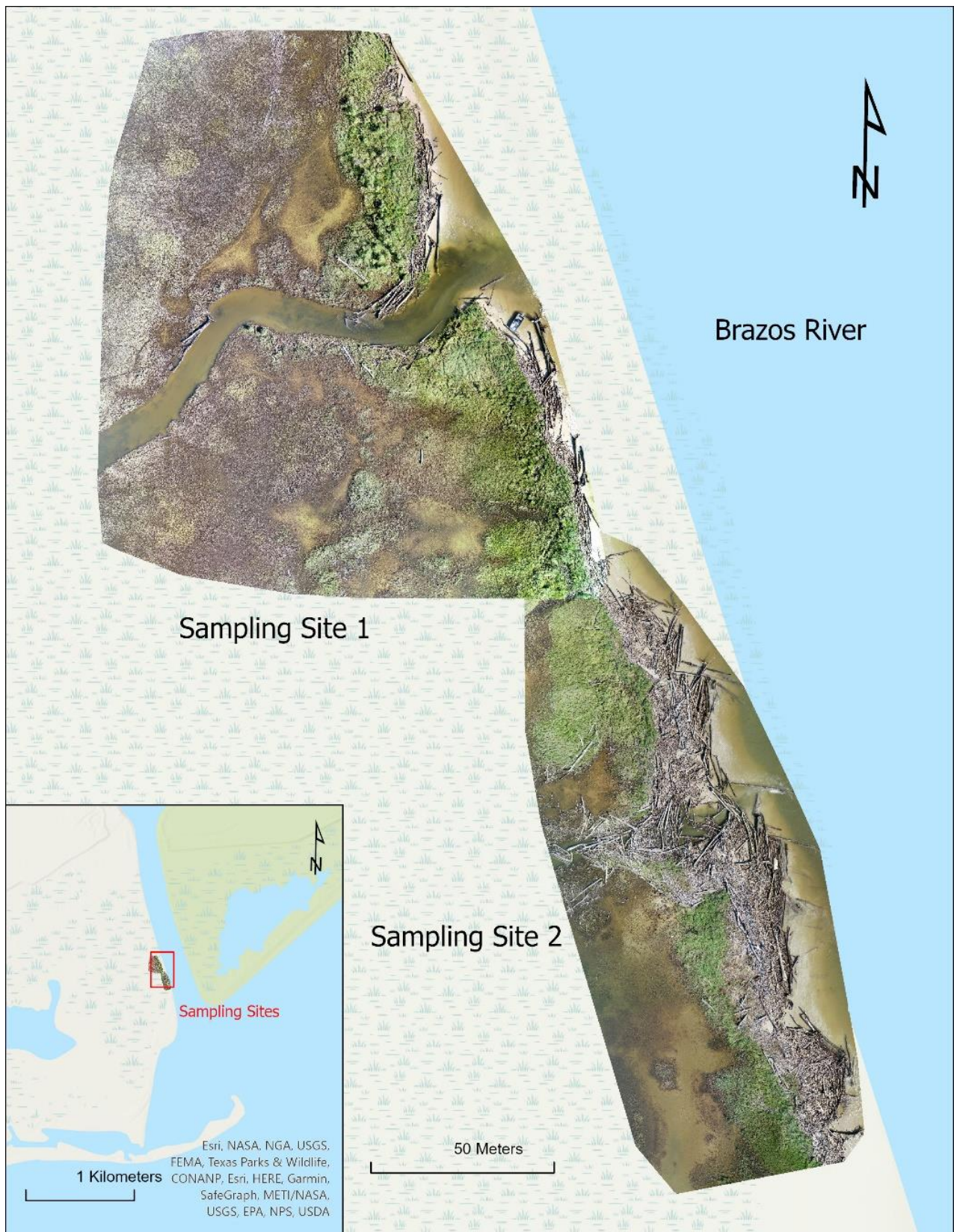


Figure 13. Sampling sites for producing orthoimages near the mouth of the Brazos river.

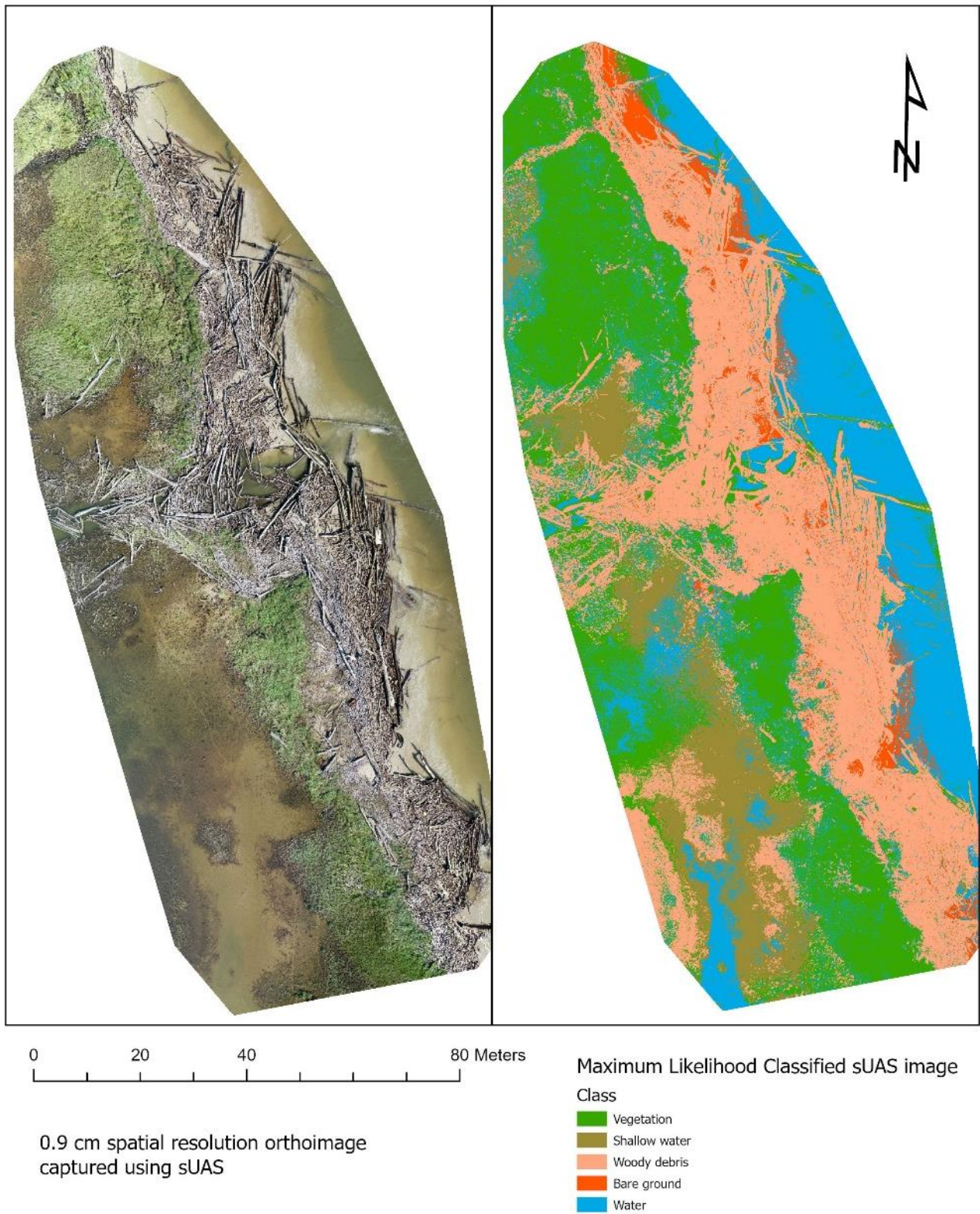


Figure 14. sUAS orthoimage and its classified image using the Maximum Likelihood classification method.

Literature Cited

- Bonner, T., J. Duke, G. Guillen, K. Winemiller, BIO-WEST. 2015. Instream Flows Research and Validation Methodology Framework: Brazos River and Associated Bay and Estuary System. Final Report to Texas Water Development Board. Contract #1400011722. September 24, 2015. 159 pages plus appendices.
- Bonner, T., J. Duke, G. Guillen, BIO-WEST. 2017. Instream Flows Research and Validation Methodology Framework 2016-2017: Brazos River and Associated Bay and Estuary System. Final Report to Texas Water Development Board. Contract #1600012009. August 2017. 450 pages plus appendices.
- Clesceri, L. S., A. E. Greenberg, and A. D. Eaton, editors. 1998. Standard Methods for the Examination of Water and Wastewater, 20th edition. American Public Health Association, American Water Works Association and Water Environment Federation, Washington, D.C.
- Dahm, C.N., Edward, R.J. and Gelwick, F.P. 2005. Gulf coast rivers of the southwestern United States, *in* Rivers of North America, Benke, A.C. and Cushing, C.E. eds. Berlington, Mass. Elsevier Academic Press.
- Dyer, K. R. 1997. Estuaries: a physical introduction, Second edition. Wiley, New York, NY. 195pages.
- Gray, J. R., G. D. Glysson, L. M. Turcios, and G. E. Schwarz. 2000. Comparability of suspended-sediment concentration and total suspended solids data. United States Geological Survey, Reston, VA. Edwards, T.K. and G.D. Glysson. 1999. Techniques of Water-Resources Investigations of the U.S. Geological Survey. Book 3, Applications of Hydraulics. Chapter C2. Field methods for measurement of fluvial sediment. U.S. Geological Survey.
- Miller, A. V. 2014. Characterization of the Brazos River Estuary. Master's Thesis. University of Houston-Clear Lake, Houston, Texas.
- Mueller, D.S. and C.R. Wagner. 2009. Measuring discharge with acoustic doppler current profilers from a moving boat. Chapter 22. Book 3. Section A. Techniques and Methods 3-A22. U.S. Geological Survey.
- Orlando, S.P., R., L.P. Rozas, G.H. Ward, and C.J. Klein. 1993. Salinity characteristics of Gulf of Mexico Estuaries. Silver Spring, MD: National Oceanic and Atmospheric Administration, Office of Ocean Resources Conservation and Assessment. 209 pp.
- Paine, J. G., S. Mathew, T. Caudle. 2011. Texas Gulf Shoreline Change Rates Through 2007. Final Report Prepared for General Land Office under contract no. 10-041-000-3737. Bureau of Economic Geology. [Texas Gulf Shoreline Change Rates through 2007 \(utexas.edu\)](http://utexas.edu)
- Renfro, W.C. 1963. Small beam net for sampling post larval shrimp. U.S. Fish and Wildlife Service Circular 161. P. 86-87.

- Savenije, H.H. 2005. Salinity and tides in Alluvial Estuaries. Elsevier Press. Amsterdam, Netherlands.
- TCEQ, 2004. Atlas of Texas Surface Waters: Maps of the classified. GI-316. 31 p. Austin, TX. Available online at: <http://www.tceq.state.tx.us/publications/gi/gi-316/index.html>.
- TCEQ. 2012. Surface Water Quality Monitoring Procedures, Volume 1: Physical and Chemical Monitoring Methods. Texas Commission on Environmental Quality, Austin, Texas.
- TCEQ. 2014. Brazos River and its Associated Bay and Estuary System [online]. Austin: Texas Commission on Environmental Quality. Environmental Flow Standards for Surface Water. Available from: <https://www.tceq.texas.gov/assets/public/legal/rules/rules/pdflib/298g.pdf>
- Vines, R.A. 1984. Trees of Central Texas. Austin, TX.